Research Article
Volume 11:3, 2022

Irrigation & Drainage Systems Engineering

ISSN: 2168-9768 Open Access

A Software for Hydraulic Analysis of Linear-move and Center-Pivot Irrigation Systems: *LincSys*, II. Application Examples and Model Evaluation

Zerihun D* and Sanchez C.A.

Maricopa Agricultural Center, University of Arizona, 37860, W. Smith-Enke Rd, Maricopa, AZ 85138-3010, USA.

Abstract

A software for simulating the hydraulics of linear-move and center-pivot irrigation systems, *LincSys*, is presented in the current paper. This manuscript is part II of a two-part paper. Descriptions of software functionalities relating to the graphical user interface and the hydraulic simulation module of *LincSys* are presented in manuscript I. Results of evaluation of the computational module are summarized and a set of application examples are presented here. A limited evaluation of the hydraulic simulation module suggests that the predictive capability of the model is satisfactory. In line with results of earlier studies, computed outputs of application examples show that the lateral pressure profiles of linear-move and center-pivot systems exhibit both local span-scale spatial variability patterns and broader inter-span trends, suggesting that a complete description of the pressure profile patterns of these laterals requires that both spatial variability attributes be assessed. While the lateral pressure spatial variability properties are primarily functions of span geometry, the outcomes of the current study confirm results from an earlier study that field slope and lateral diameter can modify the basic effects produced by span geometry. Simulated emitter discharge profiles indicate that distribution uniformity along linear-move and center-pivot laterals can be high. The results also show that, depending on the system configuration option, the spatial variability attributes of an emitter discharge profile can have similarity with certain aspects of (or can be completely different from) that of the corresponding lateral pressure profile.

Keyword: Linear-move irrigation system • Center-Pivot irrigation system • Lateral pressure profile • Emitter discharge profile • In-span variability pattern • Inter-span variability trend

Introduction

Mathematical models represent flexible and inexpensive tools for developing improved design and management of sprinkler irrigation systems, including linear-moves and center-pivots. Studies on the hydraulic modeling and design of linear-move and center-pivot systems were published by various authors. One of the first studies on center-pivot lateral hydraulics consists of the development of a step-wise approach for computing pressure distribution along a lateral with a specified outlet discharge profile [1]. Equations for the pressure head profile of a center-pivot lateral were derived considering continuous and nonuniform outflow discharge profile, constant lateral diameter, and zero slope [2]. The results presented in reference [2] were extended by taking into account the effects of constant slope and residual outflow discharge, at the distal-end, on lateral hydraulics [3]. Equations for computing friction head loss in center-pivot laterals were developed [4,5], among others. Expressions were derived for hydraulic analysis of variable diameter center-pivot laterals, based on both continuous and discrete outflow assumptions [6].

A design and evaluation model, CPED, was developed for center-pivot systems [7]. The results of a simulation study, conducted using a version of the CPED model, on variable water application with linear-move systems was reported in reference [8]. System components of linear-moves and center-pivots and design approaches and field evaluation procedures applicable to these systems are described in references [9,10].

This paper presents a software, named *LincSys*, for hydraulic simulation of center-pivot and linear-move systems. The *LincSys* software consists of a pair of executable files that are programmatically coupled: a hydraulic simulation module, *HydrSimLaterals.exe*, and a graphical user interface (GUI), *LincSys.exe*, through which the user interacts with the hydraulic module. Descriptions of software functionalities and capabilities related to the user interface and a brief discussion on the computational module are presented in part I of the current paper [11]. The current manuscript, on the other hand, presents a concise summary of the results of a limited evaluation of the hydraulic simulation module of *LincSys*, which was published as part of an earlier study by the current authors and cooperators [12]. The results suggest that model performance is satisfactory.

Furthermore, with the goal of highlighting the computational capabilities and the input-output functionalities of the model, three application examples (sample projects), one corresponding to each system configuration option of *LincSys* (i.e., Droptube-*Prv*-Emitter, Droptube-Emitter, and Emitter-On-Lateral), are presented here. The sample projects cover a wide range of lateral elevation profile, hydraulic, and geometric characteristics. The contents of the Input, Output, and Charts windows of *LincSys* corresponding to each sample project are displayed and described and differences relating to the system configuration options are highlighted. Furthermore, for each sample project a selected set of chart outputs, consisting of the energy grade-line, hydraulic grade-line, lateral pressure, *prv*-inlet pressure, *prv*-set pressure, emitter head differential (i.e., head difference across an emitter), and emitter discharge profiles are presented.

Confirming results reported by earlier studies [12,13], computed outputs of sample projects show that the lateral pressure head profiles of linear-move and center-pivot systems exhibit unique spatial variability attributes consisting of two

***Address for Correspondence:** Zerihun D, Maricopa Agricultural Center, University of Arizona, 37860, W. Smith-Enke Rd, Maricopa, AZ 85138-3010, USA, E-mail: Dawit@ag.arizona.edu*

Received: 02 March 2022, Manuscript No. idse-22-55902; **Editor assigned:** 03 March, 2022, PreQC No. P-55902; **Reviewed:** 16 March 2022, QC No. Q-55902; **Revised:** 17 March 2022, Manuscript No. R-55902; **Published:** 24 March, 2022, DOI: 10.37421/idse.2022.11.315

different forms: local span-scale variability patterns (with characteristic convex or concave forms) and broader inter-span/lateral-wide trends. The implication is that a complete description of the lateral pressure head profile variability attributes of these systems requires that both spatial variability properties be assessed. The distinct lateral pressure profile variability attributes of linear-move and center-pivot systems are primarily related to lateral geometry, however, field slope and lateral diameter have strong secondary effects that modify the basic effects produced by the span geometry. Simulated sample project outputs show that emitter discharge uniformities for linear-move and center-pivot laterals can be high, which is in line with levels reported by earlier studies [14]. Simulated sample project outputs also show that, depending on the system configuration option, the spatial variability attributes of the emitter discharge profiles can be similar to (or different from those of) the corresponding lateral pressure profiles.

Results of Model Evaluation

The current authors and cooperators have conducted a limited evaluation of the hydraulic module of *LincSys* in which computed lateral pressure head profiles and lateral inlet discharges were compared with measured data. Results of the model evaluation were published earlier by the same authors and co-operators [12], thus only a brief summary of the essential results are presented here.

Irrigation field evaluations were conducted in the spring of 2018 on a linear-move sprinkler irrigation system installed on the research farm of the Maricopa Agricultural Center of the University of Arizona, Maricopa, AZ. The linear-move system was managed by the USDA-ARS Arid-Lands Agricultural Research Center. The lateral is comprised of six spans with a concave elevation profile and a distal-end truncated cantilever type beam with a convex profile. Span lengths vary between 27.0 and 56.8 m. The lateral is operated on a level field and has an effective length of 361.7 m. The system has 349 droptube-*prv*-emtter assemblies to meter outlet discharges along the lateral. Three sets of lateral pressure head profile data, each with 32 data points suitably distributed along the lateral, were collected. Corresponding inlet discharges were also measured with digital flow meter built into the inlet support tower of the lateral. Data set 1 was used in model calibration and data sets 2 and 3 were used in model verification.

Results of model verification showed that the maximum percent absolute residuals between the simulated and measured lateral pressure head profiles are 14.3% for data set 2 and 16.0% for data set 3. The average absolute residuals of the lateral pressure head profiles are 3.7 and 3.0% for data sets 2 and 3, respectively. While the average absolute residuals suggest a reasonably good agreement between the simulated and measured pressure head profiles, the maximum absolute residuals may not be considered sufficiently small. However, a comparison of the average and maximum absolute residuals, obtained for each data-set, suggests that the maximum absolute residuals may not be good indicators of the overall error levels in the computed pressure head profiles. In fact, it can be shown that if the pair of measured pressure heads corresponding to the maximum absolute residuals are excluded from the respective pressure head profiles, the maximum absolute residual would be reduced from 14.3 to 8.8% for data set 2 and from 16.0 to 8.5% for data set 3. Furthermore, the absolute percent residuals between the measured and simulated inlet discharges were 7.5 and 3.3% for the data-sets 2 and 3, respectively, which suggests a satisfactory agreement between measurements and model predictions.

Sample projects (Application examples)

As noted in the companion paper, *LincSys* computes the link discharge and total head vectors along the lateral and a range of additional outputs, given the hydraulic, geometric, and elevation data of a linear-move or center-pivot sprinkler irrigation system as input. In order to highlight the input-output functionalities of the software and the computational capabilities of the simulation module three sample projects, one sample project corresponding to each one of the three system configuration options of *LincSys* (i.e., Droptube-Emitter, Droptube-*Prv*-Emitter, and Emitter-On-Lateral) are presented here. The sample projects consist of hypothetical lateral hydraulic simulation problems covering a wide range of lateral elevation profile and hydraulic and geometric characteristics. A summary of the input data-set for each of the sample projects (named Droptube-Emitter, Droptube-*Prv*-Emitter, and Emitter-On-Lateral) is provided in Tables 1 and 2.

Sample project for the Droptube-Emitter system configuration option

Lateral hydraulic, geometric, and slope characteristics, an overview: The Droptube-Emitter sample project (Tables 1 and 2) considers a lateral that uses drop-tubes to convey water from the lateral outlet ports down to emitters (i.e., the system has no *prvs* to regulate emitter inlet pressure). The lateral consists of a concatenated series of six concave spans and a truncated cantilever type distal-end span with a convex profile. It is operated on a field with constant negative gradient along the length of run of the lateral. The same diameter pipe is used over the six concave spans, but lateral diameter was reduced in the distal-end span. The span lengths used in this lateral are close to the upper-ends of the typical range used in linear-move and center-pivot systems, while the lateral diameter is about the average of the range commonly used in these systems.

Input data: The input data for the Droptube-Emitter sample project is displayed in the Input tabpage of *LincSys* (Figure 1a). As can be noted from the taskbar of the Input tabpage (Figure 1a), the current application example is the same as SampleProject_9 of the Droptube-Emitter system configuration option of *LincSys*. The project input data are arranged in two blocks consisting of nontabular and tabular data. The Input window displays the entire nontabular input data, but it shows only a part of the tabular input data. A summary of the input data for the current sample project is presented in Tables 1 and 2.

Each of the concave spans of the lateral, considered in the current sample project, are 61.4 m in length and the length of the distal-end span is 32.5 m (Table 1). The lateral is 400.7 m long and is installed in a field with a uniform slope of -1.5%. The maximum in-span elevation differentials are 1.5m for the concave spans and 1.0 m for the distal-end convex span. The lateral has seven support towers each 3.8 m in height. Using a horizontal surface (that passes through the lowest point in the field along the length of run of the lateral) as a reference datum, the elevation of the lateral inlet is set at 9.8m (Table 1 and Figure 1a). The total head at the lateral inlet is 20.0 m.

Lateral diameter is 162.1 mm over spans #1 to 6 and 101.6 mm in the distal-end span. The lateral has 314 outlet ports and droptube-emitter assemblies. Drop-tube lengths vary between 2.91 and 4.7 m and emitters are placed at a constant above ground clearance of 0.6m (Table 1). The emitter used in this lateral is a spray nozzle (Super spray UP3 model) with a nozzle size of 3.572mm (9/64)" from Senninger [15]. Emitter hydraulic parameters, obtained by fitting a power function to the emitter pressure-discharge data provided in manufacturer's catalogue, are summarized in Table 2. Note that, in Figure 1a, the input boxes for the *prv* hydraulic parameters are deactivated and the column for the *prv* indicator parameter, of the input data table, is set to zero, indicating that the lateral considered in the current sample project has no *prvs*.

A section of the tabular input data for the Droptube-Emitter sample project is displayed in the input data table of the Input tabpage (Figure 1a). The input data table of the current sample project is comprised of 24 columns and 640 rows. Each column of the input data table represents a data type, consisting of topological, lateral elevation, geometric, or hydraulic parameter set. On the other hand, each row of the input data table contains data related to a hydraulic link and its delimiting nodes, including nodal indexes, nodal distances and elevations, and geometric and hydraulic parameters. The horizontal and vertical scroll bars of the input data table (Figure 1a) or keys from the keyboard can be used to browse the contents of the input data table and to edit data items in the input data table cells. Details on these and the specifics of the contents of an input data table are provided in the user's manual of *LincSys*.

Output data: The output data of the Droptube-Emitter sample project is displayed in the Output window of *LincSys* (Figure 1b). The output data contains nontabular and tabular data segments. While the Output window

Table 1. Lateral hydraulic, geometric, and elevation data of sample projects

Lateral parameters		Units	Sample projects (application examples)		
			Droptube-Emitter	Droptube-Prv-Emitter	Emitter-On-Lateral
Number of spans		-	7	7	6
Span geometry	Concave	-	6	7	6
	Convex	-	1	0	0
Effective span length		m	61.4/32.5[a]	45.8	61.3
Lateral length	Horizontal	m	400	319.9	367.5
	Along centerline	m	400.7	320.5	367.9
Support tower height		m	3.8	3.2	3.8
Maximum in-span elevation differentials		m	1.5/1.0[b]	1.2	1.2
Lateral diameter		mm	162.1/101.6[c]	197.1	88.9/50.8/38.1[d]
Absolute roughness	Lateral pipe	mm	0.01	0.0015	0.003
	Drop-tube	mm	0.0015	0.0015	-
Drop-tube length range		m	2.91-4.7	2.6-3.8	-
Lateral outlet spacing		m	1.25	0.5-1.6	6.24[e]
Constant above ground clearance of emitter		m	0.6	0.6	-
Drop-tube diameter		mm	19.05	19.05	-
Field surface slope		%	-1.5	-1.8/0/-0.5[f]	0
Local head loss coefficient and related parameters	Branching, outlet	-	0.2	0.12	0.2
	Bending, connector	-	0.08	0.027	-
	Line flow	-	0.1	0.042	0.08
	Prv	-	-	1/0	-
	Span joint	-	0.3	0.3	0.3
	Valve	-	-	-	-
	Coupler	-	-	-	-
	Contraction[g]	-	0.26	-	0.34/0.195
Total head at the inlet		*m*	20	23	15
Elev. at the inlet		*m*	9.8	4.71	3.8

(a) The effective span length for the Droptube-Emitter system configuration option is 61.4 m for spans #1 to 6 and 32.5 m for the distal-end span.
(b) For the Droptube-Emitter system configuration option, the maximum in-span elevation differential is 1.5 m over spans #1 to 6 and 1.0 m for span #7. Note: the maximum in-span elevation differential considers a scenario where the span is on a level surface.
(c) Lateral diameter for the Droptube-Emitter system configuration option is 162.1 mm over the six upstream spans. It is then reduced to 101.6 mm over the distal-end span.
(d) Lateral diameter for the Emitter-On-Lateral system configuration option vary along the lateral. It is 88.9 mm over spans #1 to 4, it is then reduced to 50.8 mm over span #5, which is further reduced to 38.1 mm over the span #6.
(e) For the Emitter-On-Lateral system configuration option, the indicated lateral outlet spacing (6.24 m) is an average value.
(f) For the Droptube-Prv-Emitter sample project, the average field slope is variable.The upstream-end span is set at a slope of -1.8%. Spans #2, 3 and 4 operate on a level section of the field and spans #5, 6, and 7 run on a segment with -0.5% slope.
(g) The local head loss coefficients for sudden contraction are obtained from [19] based on area ratios.

Table 2. Emitter and *prv* data of sample projects

Lateral parameters			Units	Sample projects (application examples)		
				Droptube-Emitter	Droptube-Prv-Emitter	Emitter-On-Lateral
Number of emitters, droptube-emitter assemblies, or droptube-*prv*-emitter assemblies			-	314	330	59
Emitter data [b]	Emitter model			Super spray UP3[a]		Rainbird 30WH[a]
	Nozzle size		mm (in)	3.572 (9/64)"	5.556 (7/32)"	3.175 by 2.381 (1/8 by 3/32)
	β		L/s/m$^{\lambda}$	0.0429	0.105	0.0502
	λ		-	0.5018	0.5004	0.5182
prv data[c]	*prv* model		-	PSR2	-	
	h_{prv}		m	-	12	-
	$\delta\eta_{\pi\rho\varpi}$		m	-	3.5	-
	h_{max}		m	-	81	-

[a]Emitters used in the laterals with the Droptube-Emitter and Droptube-Prv-Emitter system configuration option are produced by Senninger [15] and those used in the Emitter-On-Lateral system configuration option are produced by Rainbird [18]. [b]β and λ are coefficient and exponent, respectively, of the emitter head-discharge function and are derived through regression from the data provided in manufacturer's catalogue. [c] the *prvs* are produced by Senninger [16], h_{prv} is *prv*-set pressure; δh_{prv} is the minimum required pressure head margin, between the *prv*- inlet pressure and h_{prv}, in order for the *prv* to operate reliably in the active mode; and h_{max} is the maximum allowable pressure at the *prv* inlet for the *prv* to operate in the active mode.

displays the entire nontabular output data, it only shows a small section of the tabular output data.

A summary of the computed emitter discharge variability data shows that emitter discharges along the lateral vary between a minimum of 0.143 L/s and a maximum of 0.1569 L/s and the average is 0.1479 L/s. On the other hand, the emitter head differential variability data shows that emitter head differential along the lateral ranges from a minimum of 11.02 m to a maximum of 13.25 m and the mean value is 11.79 m (Figure 1b). The system hydraulic performance summary shows that the emitter discharge uniformity coefficient and the low-quarter distribution uniformity are 0.975 and 0.969, respectively, which suggests a highly uniform emitter discharge distribution along the lateral.

With a uniformity coefficient of 0.951 and a low-quarter distribution uniformity of 0.939, the emitter head differential profile as well shows high uniformity. Furthermore, the output data in the additional output groupbox show that the error in the computed inlet-head estimate is 0.0016 m or 0.0082% of the imposed inlet head of 20.0 m. Figure 1b also shows that the output boxes for the *prv* operating modes are deactivated, indicating that the lateral considered here is not fitted with *prvs*.

A section of the tabular output data of the current sample project is displayed in the output data table of the Output window (Figure 1b). The full output data table of the current sample project is comprised of 20 columns and 640 rows. Each column of the output data table represents a data type, consisting of system topological or computed hydraulic parameters (including, lateral and emitter discharges, lateral pressure, local and friction head losses, hydraulic head, and total head profiles). The rows of the output data table contain data related to a hydraulic link and its delimiting nodes. Details on the specifics of the contents of the output data table and keyboard usage on how to browse through an output data table can be found in *LincSys* user's manual.

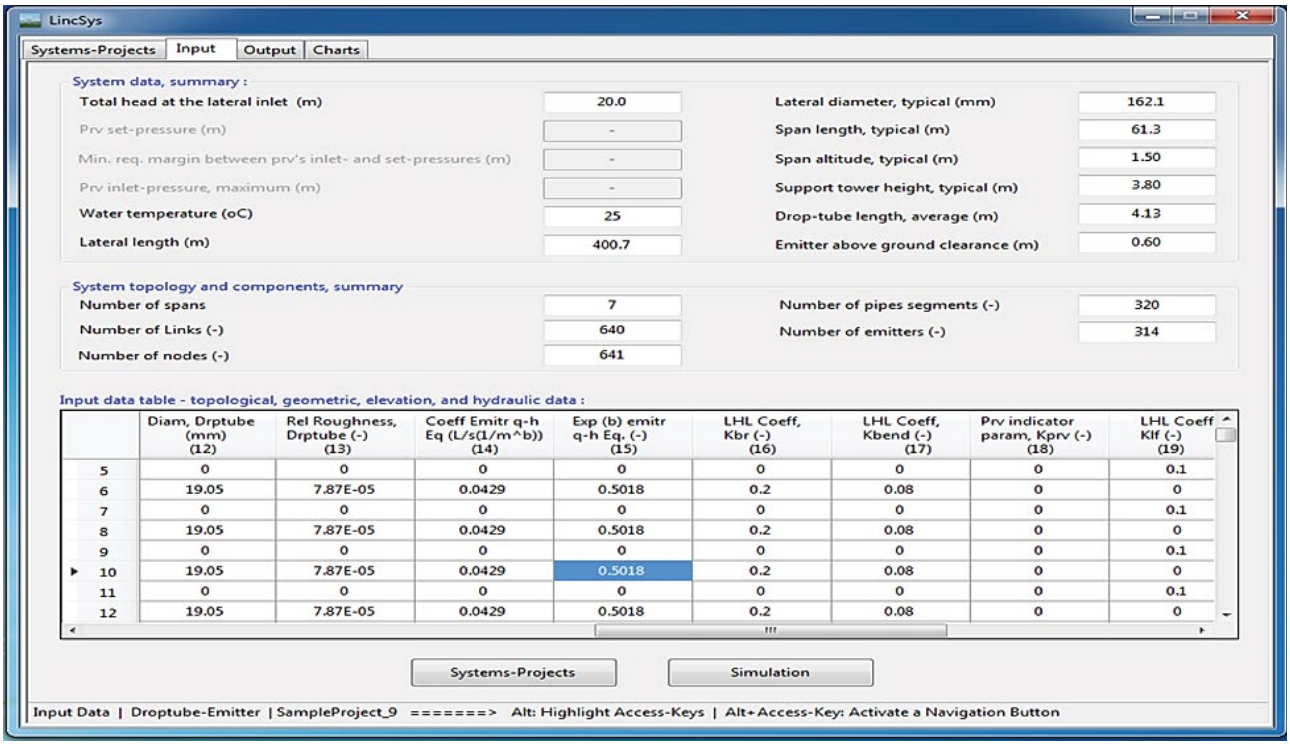

(a)

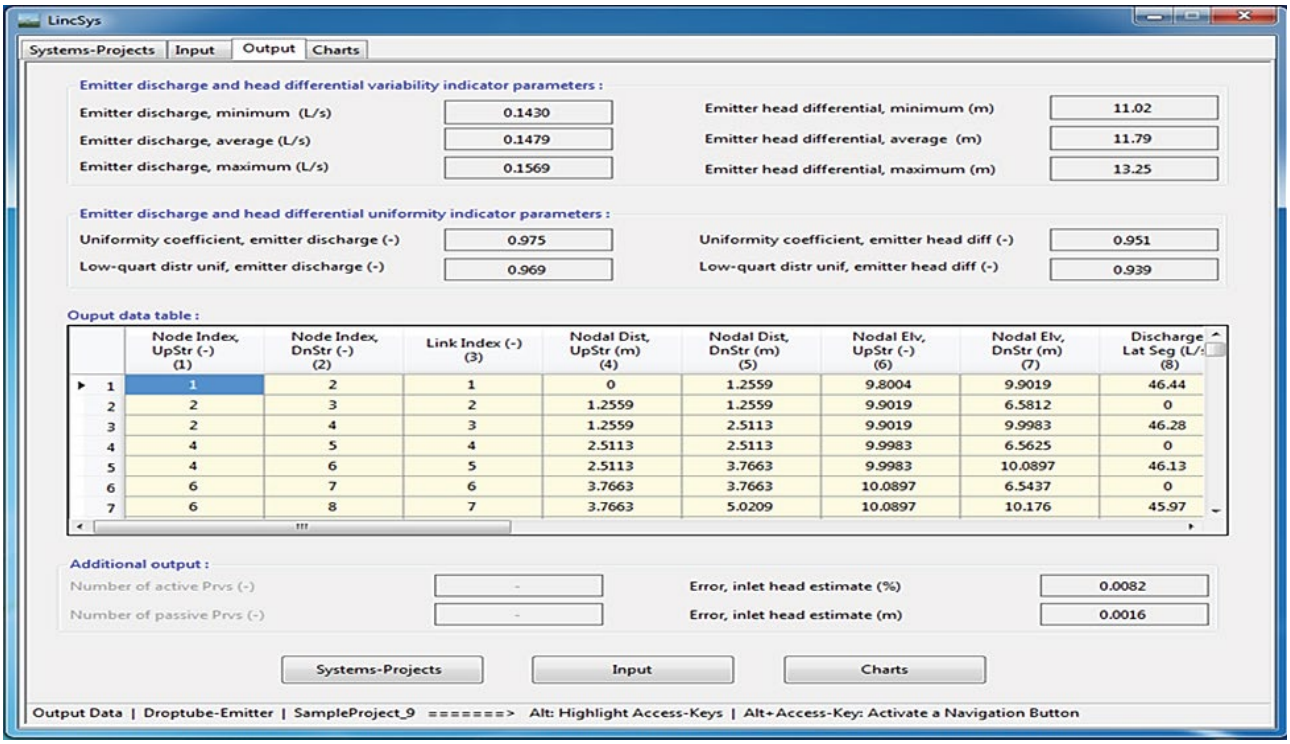

(b)

Figure 1. The Droptube-emitter sample project. (a) Input window and (b) output window

Output charts: As noted in the companion manuscript, the Charts functionality of *LincSys* produces graphs of eleven computed hydraulic parameters for the Droptube-Emitter sample project. Three of the eleven output charts, consisting of: (i) the lateral elevation profile and the hydraulic and energy grade-lines, (ii) the lateral pressure profile, and (iii) the emitter discharge profile will now be presented (Figures 2a to 2c).

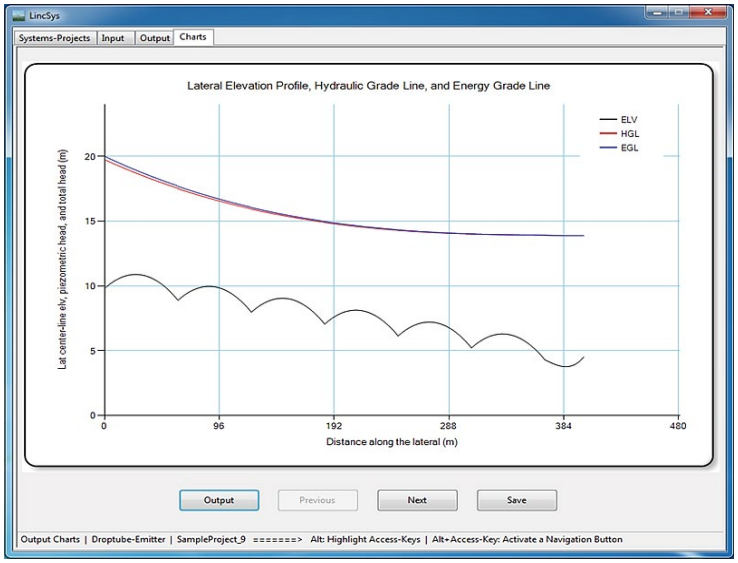

(a)

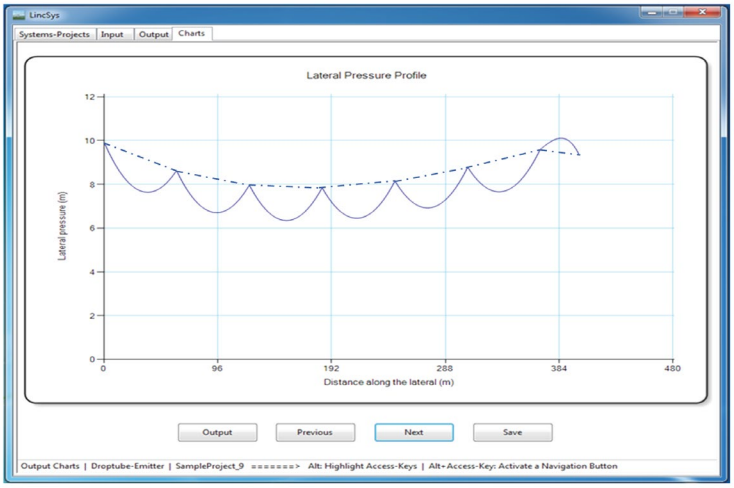

(b)

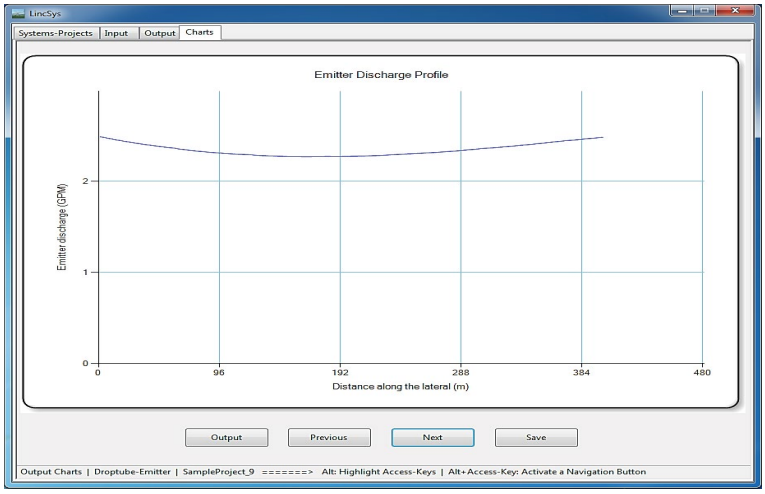

(c)

Figure 2. Charts for the Droptube-emitter sample project. (a) Lateral elevation profile and hydraulic and energy grade-lines, (b) lateral pressure profile (the solid-line represents the actual pressure head profile and the dash-dotted line depicts the inter-span variability trend), and (c) emitter discharge profile

Chart depicting the lateral elevation profile and the hydraulic and energy grade-lines: A chart showing the lateral elevation profile and the computed hydraulic and energy grade-lines for the current sample project is displayed in the Charts windows of *LincSys* (Figure 2a). The energy grade-line (i.e., the upper most curve) decreases with distance at a decreasing pace along the lateral, from a maximum of 20.0 m at the lateral inlet to 13.87 m at the distal-end of the lateral. On the other hand, the hydraulic grade-line (the curve that is right under the energy grade-line) varies between a minimum of 13.87 m at the distal-end to 19.74 m at the inlet. The total head and the hydraulic head at the distal-end appear to be identical, suggesting that the computed velocity head in the distal-end lateral pipe segment is 0m/s. However, that is not exactly correct. The computed total head and the hydraulic head at the distal-end of the lateral are different, but they appear identical only because the significant digits of the values reported here are less than those used in the numerical computation. Furthermore, the energy and hydraulic grade-lines appear to be nearly indistinct along the lateral, Figure 2a. Note that this is because of scale, in fact the data cited earlier show that the velocity head at the inlet is 0.26 m. Finally, the lower most curve, in Figure 2a, with a series of concave segments and a distal-end convex section is the elevation profile of the lateral centerline, which is installed on a field with an average slope of -1.5%.

Lateral pressure head profile chart: The lateral pressure head profile for the Droptube-Emitter sample project is depicted in solid-lines in Figure 2b. The lateral pressure head profile varies between a minimum of 6.35 m and a maximum of 10.11 m, which occurred at a distance of 154 and 385.6 m from the lateral inlet, respectively. More importantly, however, the pressure profile of the lateral exhibits both local span-scale variability patterns (solid-line) and broader inter-span/lateral-wide trends (shown in dash-dotted line), which is consistent with results of earlier studies. A more detailed discussion on in-span pressure variability patterns and inter-span trends and their relationship with span geometry, field slope, and lateral diameter is provided in reference [13]. Thus, only a brief description appertaining to the pressure head profile patterns of the current sample project will be presented here.

As can be noted from Figure 2b, the in-span lateral pressure profile variability patterns exhibit some general attributes that are repeated along the lateral, although with some variation. For the six (upstream) concave spans the corresponding local in-span lateral pressure head variability patterns invariably follow a convex form, consisting of an upstream section over which pressure decreases with distance from the lateral inlet to a local minimum somewhere within the span and a downstream section over which pressure increases with distance from the lateral inlet. By comparison, over the distal-end span (i.e., a span with a convex elevation profile), the in-span pressure variability pattern exhibits a concave form. Thus, the lateral pressure profiles show an increasing trend over an upstream section of the span, followed by a decreasing trend in the lower section of the span.

The pressure differentials across individual spans (i.e., the difference between a span's inlet and distal-end pressures), when considered over two or more consecutive spans, yield a broader trend in pressure variability over multiple spans and across a lateral. Such a pressure variability attribute is referred here as the inter-span lateral pressure variability trend [12] and is shown in Figure 2b with a dash-dotted line. The actual pressure profiles of linear-move laterals exhibit relatively complex spatial variability attributes. As a result, the broader inter-span/lateral-wide trends inherent in them may not be readily discernible. Thus, a simpler curve obtained by connecting the pressure heads at the inlet- and distal-ends of each span can be used to represent the inter-span/lateral-wide pressure variability trends along a lateral. The goal is to use the readily discernible and distinct monotonic properties of such a curve to characterize the overall spatial variability attributes of pressure over an entire lateral or a section of it encompassing one or more consecutive spans. Note that, in Figure 2b, the lateral pressure profile computed with *LincSys* consists, only, of the curve shown in solid-line, while the curve representing the inter-span trend is added manually.

A close look at Figure 2b reveals that over the upper 184.1 m section of the lateral, i.e., over spans #1 to 3, the inter-span pressure variability trends down as one moves downstream from the lateral inlet. Thereafter, over spans #4 to 6 (i.e., over a segment of the lateral measuring 184.1 m), the inter-span pressure variability tends upwards with distance from the lateral inlet. The results of an earlier study [13] suggests that the inter-span lateral pressure variability trend observed over the six upstream spans, in Figure 2b, are mainly attributable to the field slope, which is -1.5%.

Now, considering spans #6 and 7, the inter-span pressure variability trend changed slightly from one of increasing with distance along the lateral (in span #6) to that of decreasing in span #7. This change in the inter-span trend is related to changes in the span concavity structure and, to some extent, in the lateral diameter over span #7. Span geometry changed from concave (over the six upstream spans) to convex form over the distal-end span and lateral diameter was reduced from 162.1mm (over the upstream spans) to 101.6mm over the distal-end span. As can be noted from Figure 2b, these changes, in span geometry and diameter, did have a discernible effect on the overall inter-span pressure variability trend.

Emitter discharge profile chart: A chart showing the emitter discharge profile for the current sample project is depicted in Figure 2c. The emitter discharge profile exhibits a spatial trend that is analogous in form to the overall inter-span lateral pressure variability trend described in the preceding paragraph. It decreased with distance from the lateral inlet over the upper 165.3 m section of the lateral, it then rose with distance from the inlet-end in the lower 235.4 m long segment of the lateral.

Remarkably, the emitter discharge profile depicted in Figure 2c is a nearly smooth and almost convex function of distance from the later inlet. In other words, the effects of span-scale elevation differentials are not as evident in the emitter discharge profile as they are in the lateral pressure profile. The explanation for this observation relates to the position of emitters with respect to the lateral centerline and the spatial invariance of emitter's above ground clearance along the lateral.

In the lateral considered in current sample project, emitters are placed at a significantly lower elevation relative to the lateral outlet ports. As a result, emitter pressures on the average exceed the respective lateral outlet pressures by 4.1 m, which is about the average length of the drop-tubes. Thus, in this lateral, emitter inlet pressure heads are not only different from the corresponding lateral outlet pressure heads, but they are also appreciably larger. Furthermore, owing to the positioning of emitters at a uniform above ground clearance from the field surface, the pressure differentials between emitters and those of the respective lateral outlets vary in a pattern that nearly even-out the in-span elevation differential effects on emitter pressure heads. Consequently, the rather pronounced span-scale wiggles in the lateral pressure profile, which are attributable to the in-span lateral elevation differential effects, are barely discernible on the corresponding emitter discharge profile (Figure 2c).

Sample project for the Droptube-Prv-Emitter system configuration option

Lateral hydraulic, geometric, and slope characteristics, an overview: The Droptube-*Prv*-Emitter sample project considers a system that uses drop-tubes to convey water from the lateral outlet ports down to *prv*-emitter assemblies. A summary of the lateral hydraulic and geometric data and the slope of the field on which the system is installed are provided in Tables 1 and 2. The system considered in the current sample project has seven concave spans and is installed on a field with variable slope along the length of run of the lateral. The lengths of the spans used in this lateral are shorter than the average span lengths of typical linear-move and center-pivot systems. By comparison, the lateral diameter, which is constant along the lateral, is close to the upper limit of the range commonly used in these systems.

Input data: The contents of the Input window of *LincSys* for the current sample project are depicted in Figure 3a. The Input window displays both the nontabular and tabular input data for the Droptube-*Prv*-Emitter sample project. As can be noted from the taskbar of the Input tabpage (Figure 3a), the current application example is the same as SampleProject_5 of the Droptube-*Prv*-Emitter system configuration option of *LincSys*.

The length of the lateral considered in the current sample project is 320.5 m and each span of the lateral is 45.8 m long (Figure 3a and Table 1). The lateral is operated on a field with variable slope. The upstream-end span is set on a slope of -1.8%, spans #2, 3, and 4 operate on a level section of the field, and spans #5, 6, and 7 run on a segment of the field with -0.5% slope. The maximum in-span elevation differential, if the lateral were to run on a level field is 1.2 m. The lateral has eight support towers each 3.2 m in height. Using a horizontal surface that passes through the point of minimum field elevation

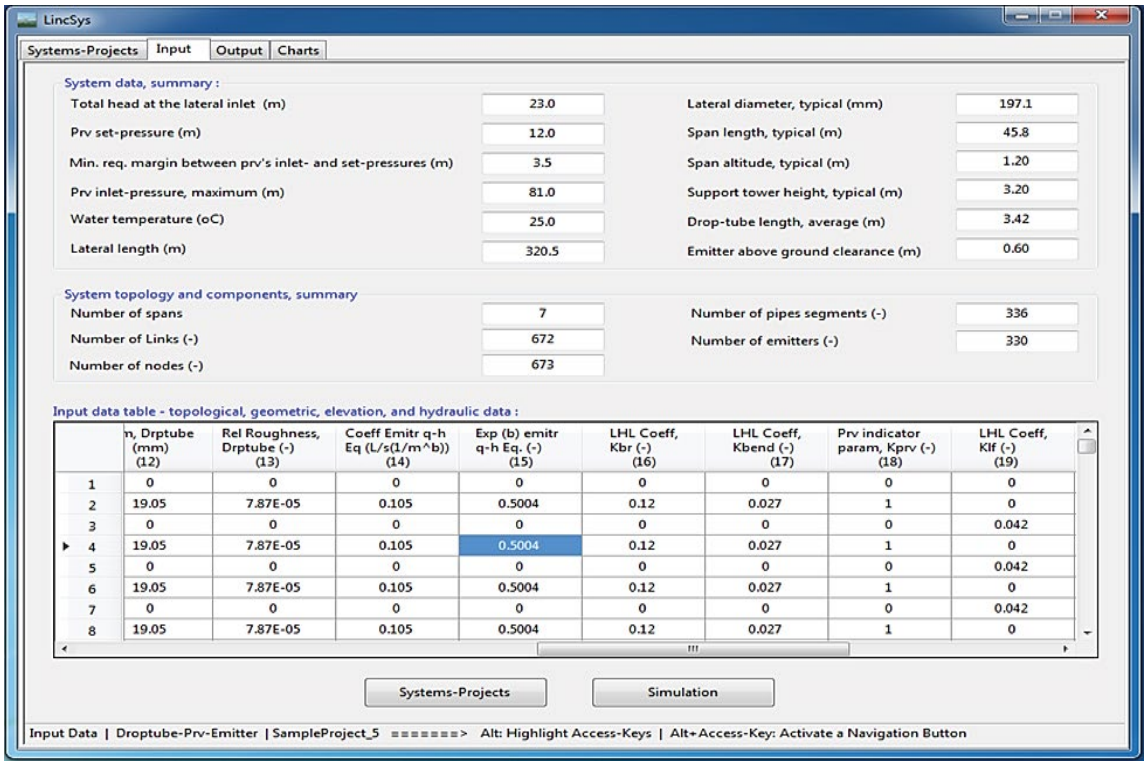

	n, Drptube (mm) (12)	Rel Roughness, Drptube (-) (13)	Coeff Emitr q-h Eq (L/s(1/m^b)) (14)	Exp (b) emitr q-h Eq. (-) (15)	LHL Coeff, Kbr (-) (16)	LHL Coeff, Kbend (-) (17)	Prv indicator param, Kprv (-) (18)	LHL Coeff, Klf (-) (19)
1	0	0	0	0	0	0	0	0
2	19.05	7.87E-05	0.105	0.5004	0.12	0.027	1	0
3	0	0	0	0	0	0	0	0.042
4	19.05	7.87E-05	0.105	0.5004	0.12	0.027	1	0
5	0	0	0	0	0	0	0	0.042
6	19.05	7.87E-05	0.105	0.5004	0.12	0.027	1	0
7	0	0	0	0	0	0	0	0.042
8	19.05	7.87E-05	0.105	0.5004	0.12	0.027	1	0

(a)

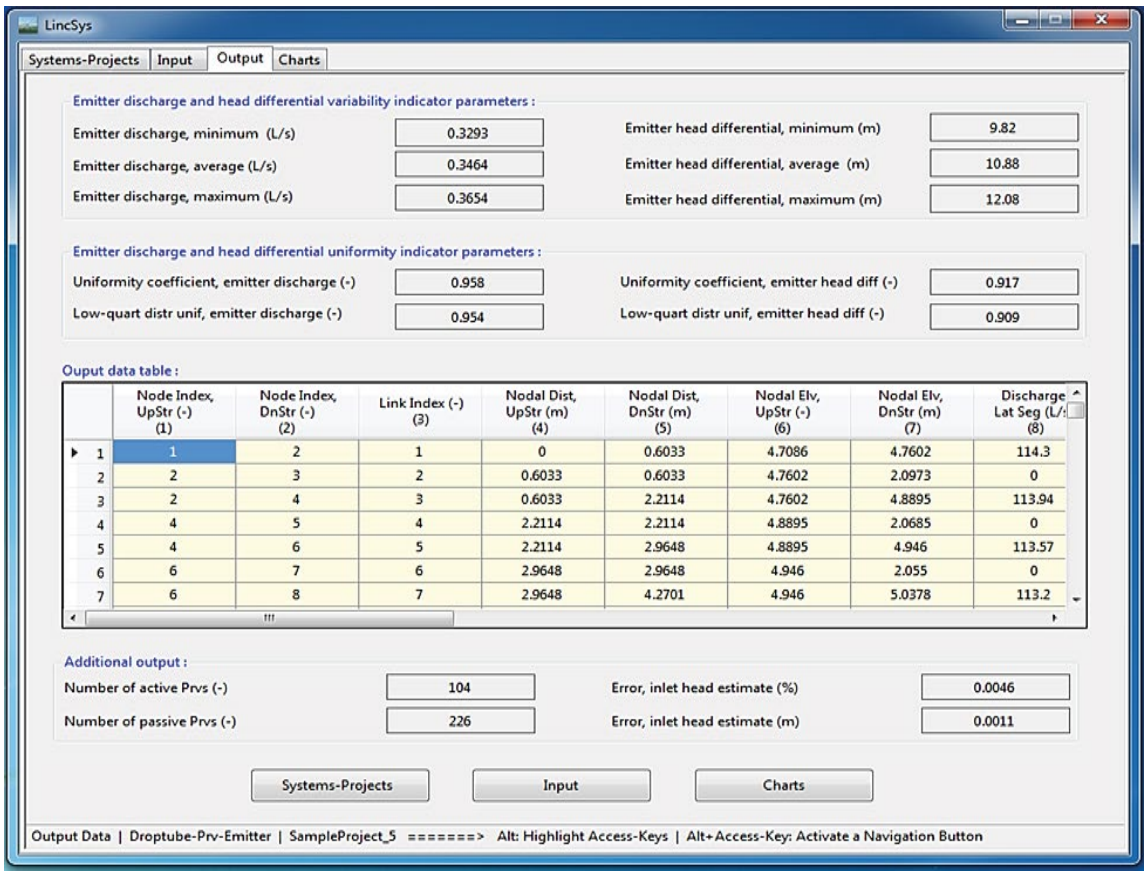

	Node Index, UpStr (-) (1)	Node Index, DnStr (-) (2)	Link Index (-) (3)	Nodal Dist, UpStr (m) (4)	Nodal Dist, DnStr (m) (5)	Nodal Elv, UpStr (-) (6)	Nodal Elv, DnStr (m) (7)	Discharge Lat Seg (L/s (8)
1	1	2	1	0	0.6033	4.7086	4.7602	114.3
2	2	3	2	0.6033	0.6033	4.7602	2.0973	0
3	2	4	3	0.6033	2.2114	4.7602	4.8895	113.94
4	4	5	4	2.2114	2.2114	4.8895	2.0685	0
5	4	6	5	2.2114	2.9648	4.8895	4.946	113.57
6	6	7	6	2.9648	2.9648	4.946	2.055	0
7	6	8	7	2.9648	4.2701	4.946	5.0378	113.2

(b)

Figure 3. The Droptube-Prv-Emitter sample project. (a) Input window and (b) output window

along the length of run of the lateral as the reference datum, the elevation of the lateral inlet is set to 4.71 m. The total head at the lateral inlet is 23.0 m (Figure 3a).

Lateral diameter is 197.1 mm. The lateral has 330 outlet ports, drop-tubes, and *prv*-emitter assemblies each (Table 2 and Figure 3a). Drop-tube lengths vary in the range 2.6 to 3.8 m and the constant above ground clearance of emitters is 0.6 m. The emitter used in this lateral is a spray nozzle (Super spray UP3 model) with a nozzle size of 5.556 mm (7/32)" from Senninger [15]. The emitter hydraulic parameters are summarized in Table 2. The model of the *prv* used in the lateral is PSR2 and is produced by Senninger [16]. The *prv*-set pressure, the maximum allowable inlet pressure for the *prv* to operate reliably in the active mode, and the minimum required pressure head margin between the *prv*-inlet pressure and the *prv*-set pressure for the *prv* to operate reliably in the active mode are given in Figure 3a and also Table 2.

A section of the tabular input data is displayed in the input data table of the Input window (Figure 3a). The input data table of the current sample project has 24 columns and 672 rows. In contrast to the input data table of the Droptube-Emitter sample project (where the entire column of the *prv* indicator parameters is set to zero), for the current sample project the even-numbered rows of the *prv* indicator parameter column are set to 1 (Figure 3a), indicating that the lateral considered in the current sample project is fitted with *prvs*.

Output data: The output data for the Droptube-*Prv*-Emitter sample project are displayed in the Output window of *LincSys* (Figure 3b). A summary of the emitter discharge variability data shows that emitter discharges along the lateral vary between a minimum of 0.3293 L/s and a maximum of 0.3654 L/s and the average is 0.3464 L/s. The data also shows that the emitter head differential along the lateral ranges between 9.82 and 12.08 m, with a mean value of 10.88 m. The system hydraulic performance summary shows that with a uniformity coefficient of 0.958 and a low-quarter distribution uniformity 0.954, the computed emitter discharge profile along the lateral can be considered highly uniform (Figure 3b). The uniformity coefficient and low-quarter distribution uniformity of the emitter head differential profile are 0.917 and 0.909, respectively, which also suggests a high degree of uniformity. Furthermore, the output data in the additional output groupbox show that 104 of the 330 *prvs* are operating in the active mode and the remaining 226 *prvs* are operating in the passive mode and the error in the computed inlet-head estimate is 0.0011m or 0.0046% of the imposed inlet head of 23.0 m.

A section of the tabular output data of the sample project is displayed in the output data table of the Output tabpage (Figure 3b). The tabular output of the current sample project has 20 columns and 672 rows. Each column of the output data table represents a data type consisting of lateral topological, elevation, and computed hydraulic parameters and each row contains a data-set related to a hydraulic link and its delimiting nodes.

Output charts: Among the eleven output charts of the current sample project, generated by *LincSys*, a set of three charts depicting: (i) the lateral pressure head profile, (ii) the emitter head differential, *prv*-inlet pressure, and *prv*-set pressure profiles, and (iii) the emitter discharge profile are presented here (Figures 4a to 4c).

Lateral pressure profile chart: The lateral pressure profile for the Droptube-*Prv*-Emitter sample project is shown in Figure 4a. The lateral pressure head profile ranges between 9.83 and 17.58 m, occurring at a distance of 250.9 m from the lateral inlet and the inlet end of the lateral, respectively. As was the case with the Droptube-Emitter sample project, the lateral pressure profile of the current sample project also exhibits both in-span (shown in solid-line) and inter-span trends (depicted in dash-dotted line). A close look at Figure 4a shows that the inter-span pressure variability trends down, but at a decreasing rate, over spans #1 to 5 and then inches slightly upwards over spans #6 and 7 as one moves downstream along the lateral. The main explanatory factor for the slight rise in the inter-span pressure variability trend curve observed over spans #6 and 7 is the field slope, which has a negative gradient over the spans #5 to 7. Additional discussion on the relationship between the inter-span pressure variability trends and field slope is provided in reference [13].

Chart depicting the emitter head differential, *Prv*-inlet pressure, and *Prv*-set pressure profiles: Figure 4b depicts the profiles of the *prv*-set pressure along with the computed emitter head differential and *prv*-inlet pressure for the current sample project. The upper most curve is the *prv*-inlet pressure profile. The lower most curve is the emitter head differential profile and the horizontal line in between is the *prv*-set pressure profile, which is constant at 12.0 m. The inlet pressure at the upstream-end *prv* is 20.42 m, which is well above the minimum required for the *prv* to operate reliably in the active mode, i.e., 15.5 m. Note that the minimum required *prv*-inlet pressure is the sum of the *prv*-set pressure (12 m) and the minimum required margin for an active *prv* between the *prv*-inlet and *prv*-set pressure, which is 3.5 m

As can be noted from Figure 4b, the *prv*-inlet pressure generally trends down with distance from the lateral inlet. It falls under the 15.5 m mark at a distance of 101.5 m from the inlet and thereafter it continues to decline at a decreasing pace (overall) over the next 127.9 m segment of the lateral. Then, the *prv*-inlet pressure inches slightly upwards over the lower 91.1 m section (i.e., over spans #6 and 7) of the lateral, mainly because of the negative gradient of the field that this section of the lateral is installed in. Nonetheless, the *prv*-inlet pressure profile stays under 15.5 m over the lower 219.0 m reach of the lateral.

The implication is that over the upper 101.5 m section of the lateral (which contains 104 of the 330 *prv*-emitter assemblies in the lateral) the *prv*-inlet pressures are at least equal to the minimum required inlet pressure for an active *prv*. Considering that the maximum allowable *prv*-inlet pressure is 81.0 m (Table 2), which exceeds the computed maximum *prv*-inlet pressure of 20.42 m, it can be readily observed that in the upper 101.5 m reach of the lateral, the *prv*-inlet pressure varies within the range required for the *prv* to operate reliably in the active mode (i.e., between a minimum of 15.5 m and a maximum of 81.0 m). It, thus, follows that the *prvs* in this lateral segment operate in the active mode and hence the corresponding emitter pressure heads are constant at the *prv*-set pressure [17]. As a result, in Figure 4b the *prv*-set pressure and the emitter head differential profiles are overlapped over this section of the lateral. By comparison, over the lower 219.0 m reach of the lateral the *prv*-inlet pressures are less than the minimum required for an active *prv* (i.e., 15.5 m). Consequently, the emitter head differentials, over this segment of the lateral, are less than the corresponding *prv*-set pressures (Figure 4b) and hence all the 226 *prvs* there are operating in the passive mode.

Notably, the *prv*-inlet pressure profile is a nearly smooth and almost convex function of distance from the lateral inlet (Figure 4b). In other words, the effects of the in-span elevation differentials, on the *prv*-inlet pressure profile, are not as evident as they are in the lateral pressure head profile. The explanation for this observation relates to the position of the *prvs* relative to the lateral centerline and the spatial invariance of the *prv*-emitter above ground clearance.

Because of the positions of the *prv*-emitter assemblies relative to the lateral centerline, the *prv*-inlet pressures are significantly greater than the corresponding lateral outlet pressures. For instance, the lateral-wide average pressure differential between the *prv*-inlets and the respective lateral outlets, for the current sample project, is about 3.2 m (which is nearly the same as the average droptube length of 3.4 m). Furthermore, because of the positioning of the *prv*-emitter assemblies at a uniform above ground clearance from the field surface, the pressure head differentials between the *prv*-inlets and the respective lateral outlets vary in a pattern that nearly even-out the in-span elevation differential effects on the *prv*-inlet pressure head profile. Consequently, the more pronounced span-scale wiggles of the lateral pressure profile (Figure 4a) are barely discernible in the *prv*-inlet pressure profile (Figure 4b).

Furthermore, over the lower 219.0 m segment of the lateral where *prvs* are operating in the passive mode (and hence the corresponding emitters interact directly with the flow dynamics upstream of the *prv*), the emitter head differential profile shows a spatial variability pattern that is analogous in form to that of the *prv*-inlet pressure profile. Given that (for *prvs* operating in the passive mode) the emitter head differential differs from the *prv*-inlet pressure by a constant amount (an amount equal to the required pressure head margin between the *prv*-inlet pressure and the *prv*-set pressure, 3.5 m), it stands to reason that these profiles exhibit a similar spatial pattern over the lower 219.0 m section of the lateral..

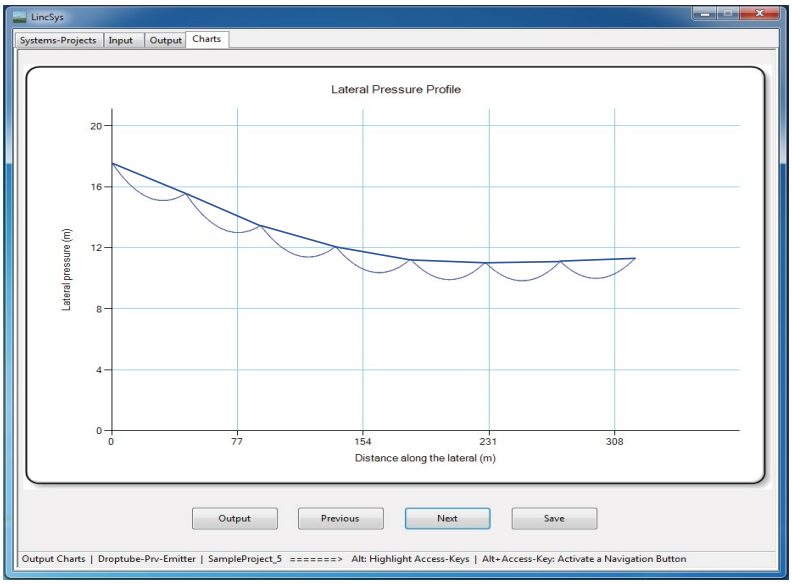

(a)

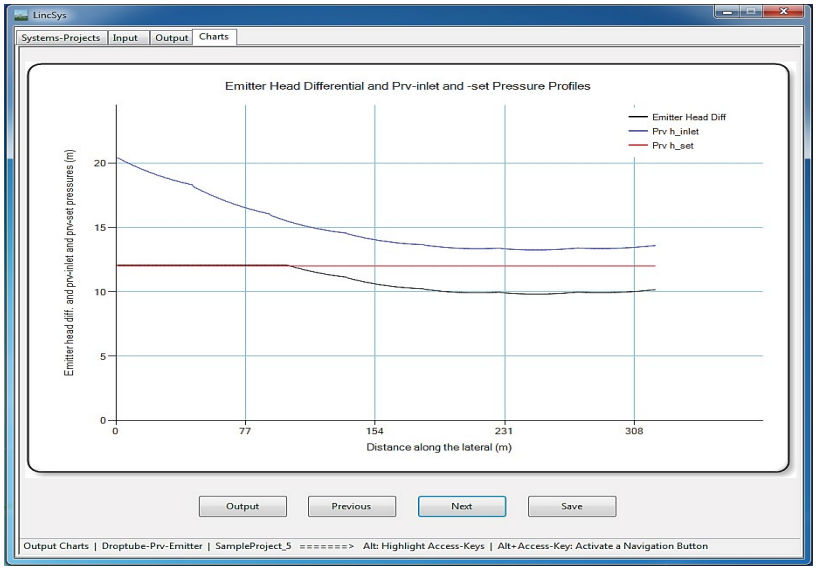

(b)

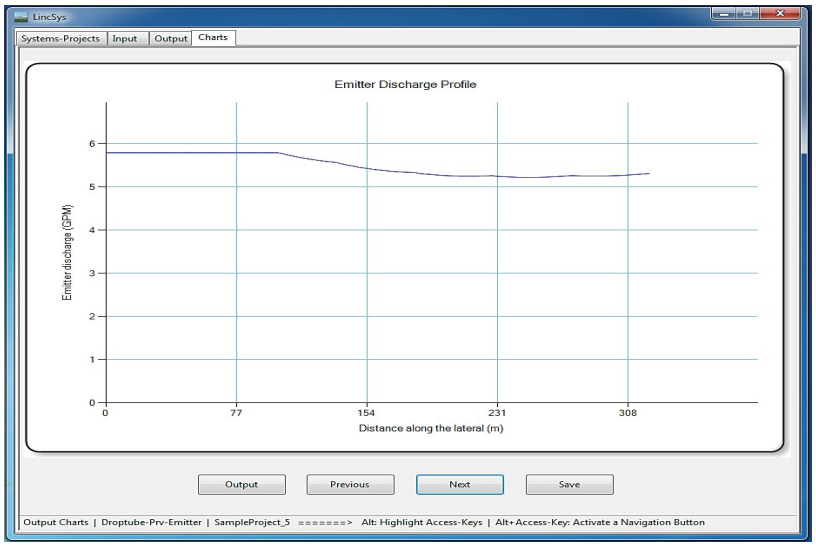

(c)

Figure 4. Charts of the Droptube-Prv-Emitter sample project. (a) Lateral pressure profile (the solid-line represents the actual pressure head profile and the dash-dotted line depicts the inter-span variability trend), (b) Prv-inlet pressure, Emitter head differential, and Prv-set pressure profiles, and (c) emitter discharge profile

Emitter discharge profile chart: The emitter discharge profile for Droptube-*Prv*-Emitter sample project is depicted in Figure 4c. A closer look at the emitter discharge profile reveals that it is analogous in form to that of the emitter head differential profile (Figure 4b). It is constant at 5.792GPM (0.3654 L/s) over the upper 101.5 m segment of the lateral (which is the segment of the lateral in which *prvs* are operating in the active mode) and thereafter it generally trends down with distance from the lateral inlet over the next 127.9 m segment of the lateral. It then inches slightly upwards over the distal 91.1 m section (i.e., spans # 6 and 7) of the lateral. Nonetheless, emitter discharge over the lower 219.0 m reach of the lateral stays under the discharge level corresponding to the *prv*-set pressure.

Note that the slight wiggles evident in the emitter discharge profile over the lower 219.0 m section of the lateral (Figure 4c) represent traces of the effects of the span geometry on the emitter discharge profile, as was the case with the emitter head differential profile (Figure 4b). Given that emitter discharge is a direct function of emitter head differential, it can be readily observed that the similarity in the spatial patterns of the emitter head differential and emitter discharge profiles is consistent with intuitive reasoning.

Sample project for emitter-on-lateral system configuration option

Lateral hydraulic, geometric, and slope characteristics: an overview: The Emitter-On-Lateral sample project considers a lateral in which emitters are placed directly on the lateral outlet ports. A summary of the lateral hydraulic and geometric parameters and the slope of the field on which the lateral is operated is provided in Tables 1 and 2. The system parameters summary show that the lateral considered here runs on a level field and consists of six concave spans with variable pipe diameter. The span length of this lateral is close to the upper limit of the range commonly used in linear-move and center-pivot systems.

Input data: The Input data for the Emitter-On-Lateral sample project are displayed in the Input tabpage of *LincSys* (Figure 5a). As can be noted from the taskbar of the Input tabpage (Figure 5a), the current application example is the same as SampleProject_15 of the Emitter-On-Lateral system configuration option of *LincSys*.

Each span of the lateral considered here is 61.3 m in length and has 1.2 m altitude (Figure 5a and Table 1). The lateral is 367.9 m in length and is supported by seven wheeled towers, each 3.8 m in height. Using the field surface as the reference datum, the elevation of the lateral inlet is set to 3.8 m. The total head at the lateral inlet is 15.0 m. Pipe diameter varies along the lateral, a diameter of 88.9 mm was used over spans #1 to 4, which is then reduced to 50.8 mm in span #5 and to 38.1mm over span #6 (Table 1). A total of 59 outlet ports, with an average emitter spacing of 6.24 m, are used to distribute water along the length of the lateral (Tables 1 and 2). Emitters used in the current lateral, which are placed directly on the outlet ports, are high pressure impact sprinklers (30WH model) with a spreader nozzle (nozzle size of 3.175 by 2.381mm [1/8 by 3/32]") from [18]. The emitter hydraulic parameters are summarized in Table 2. Note that the input data boxes for the *prv* hydraulic parameters are deactivated (Figure 5a), because the lateral considered in the current sample project is not fitted with *prvs*. In addition, input boxes for the average drop-tube length and emitter above ground clearance are also deactivated, indicating that the lateral has no drop-tubes and the above ground clearance of emitters is not constant along the lateral.

A section of the tabular input data (the input data table) for the Emitter-On-Lateral sample project is displayed in the Input window of *LincSys* (Figure 5a). The complete input data table for the current sample project consists of 24 columns and 588 rows. Note that the drop-tube parameter columns (columns 11 to 13), the column for the local head loss coefficient associated with bending losses, and the *prv* indicator parameter columns (i.e., columns #17 and 18, respectively) are set to zero, indicating that the lateral considered in the current sample project is not fitted with drop-tubes and *prvs*. Descriptions of the columns and rows of the input data table and keyboard usage on how to browse and edit the contents of the input data table are described in the user's manual of *LincSys*.

Output data: The output data for the current sample project are displayed in the Output window of *LincSys* (Figure 5b). The computed emitter discharge variability data show that emitter discharges vary over a relatively wider range, between a lower limit of 0.1191 L/s and an upper limit of 0.1708 L/s, the average being 0.1462 L/s. The emitter head differentials as well vary over a wide interval ranging from 5.3 to 10.62 m and the mean value is 7.92 m. The system hydraulic performance summary indicates that the emitter discharge uniformity coefficient is 0.927 and the low-quarter distribution uniformity is 0.869, which suggests a fairly high emitter discharge distribution uniformity along the lateral (Figure 5b). With a uniformity coefficient of 0.862 and a low-quarter distribution uniformity of 0.758, the emitter head differential profile is rather less uniform compared to the discharge profile. Furthermore, the error in the computed inlet-head estimate is 0.0009 m or 0.0057% of the imposed inlet head of 15.0 m.

A section of the tabular output data for the Emitter-On-Lateral sample project are displayed in the Output tabpage of *LincSys* (Figure 5b). The output data table of the sample project consists of 20 columns and 588 rows. A description of the columns and rows of the output data table are provided in the user's manual of *LincSys*.

Output charts: Among the eleven output charts of the current sample project produced by *LincSys*, sample charts consisting of: (i) the lateral elevation profile and the computed lateral hydraulic and energy grade-lines, (ii) the lateral pressure profile, and (iii) the emitter discharge profile are presented in Figures 6a to 6c.

Chart depicting the lateral elevation profile and the hydraulic and energy grade-lines: A chart showing the lateral elevation profile and the computed hydraulic and energy grade-lines for the Emitter-On-Lateral sample project is displayed in the Charts windows of *LincSys* (Figure 6a). As can be noted from Figure 6a, the energy grade-line (i.e., the upper most curve) decreased with distance along the lateral from a maximum value of 15.0 m at the lateral inlet to 10.15 m at the distal-end of the lateral. The hydraulic grade-line (which is right under the energy grade-line) varies between a minimum of 10.15 m at the distal-end to 14.9 m at the inlet. Although the data suggest that the velocity head at the distal-end is zero, that is not actually the case. It appears so, only because of differences in the significant digits, used in numerical computations and, of the data presented here. Furthermore, the energy and hydraulic grade-lines appear to be indistinct along the lateral, Figure 6a. However, that is only because of scale, in fact the data presented above show that the velocity head at the inlet is 0.1 m.

Note that both the energy and the hydraulic grade-lines have three segments. Over the upper 245.2 m segment (covering spans #1 to 4) of the lateral both parameters decrease with distance from the lateral inlet at a decreasing rate. However, in the upper reach of span #5, the trend in the rate of decline observed in the upstream spans is reversed and both the energy and hydraulic grade-lines begin to decrease at a faster pace with distance from the lateral-inlet, although it can be noted that the rate of decrement slows down with distance within span #5. Once again in the upper section of span #6, the rate of decrement in both the energy and hydraulic grad-lines tend to accelerate compared to the lower section of span #5. Evidently, the observed pattern of variability in the lower reaches of the energy and hydraulic grade-lines is related to the progressive decrement in lateral diameter from 88.9 mm over spans #1 to 4 to 50.8 mm in span #5 and then to 38.1 mm in span #6. In Figure 6a, the lower most curve, with a series of concave segments, represents the elevation profile of the lateral centerline, which shows that the lateral is installed on a level field.

Lateral pressure profile chart: The lateral pressure profile for the current sample project is depicted in Figure 6b. Lateral pressure profile varies between a minimum of 5.28 m and 11.1 m, occurring at a distance of 340.3 m from the lateral inlet and at the lateral inlet, respectively. Consistent with the results described earlier for the other sample projects, here as well the lateral pressure profile exhibits both in-span and inter-span trends. A closer look at Figure 6b shows that the inter-span pressure variability trends down over spans #1 to 4, but at a decreasing rate, as one moves downstream from the lateral inlet (which is consistent with the fact that the lateral is installed on a level field). By contrast, over spans #5 and 6 the inter-span pressure variability continue to trend down as one moves in the downstream direction, but at an accelerated pace compared to spans upstream, which evidently is related the progressive reduction in lateral diameter over these spans.

Emitter discharge profile chart: The emitter discharge profile for the

Emitter-On-Lateral sample project is shown in Figure 6c. The emitter discharge varies from 0.1191 to 0.1708 L/s, occurring at a distance of 344.1 m from the lateral inlet and the lateral inlet, respectively. In contrast to the Droptube-Emitter and Droptube-*Prv*-Emitter sample projects, the emitter discharge variability

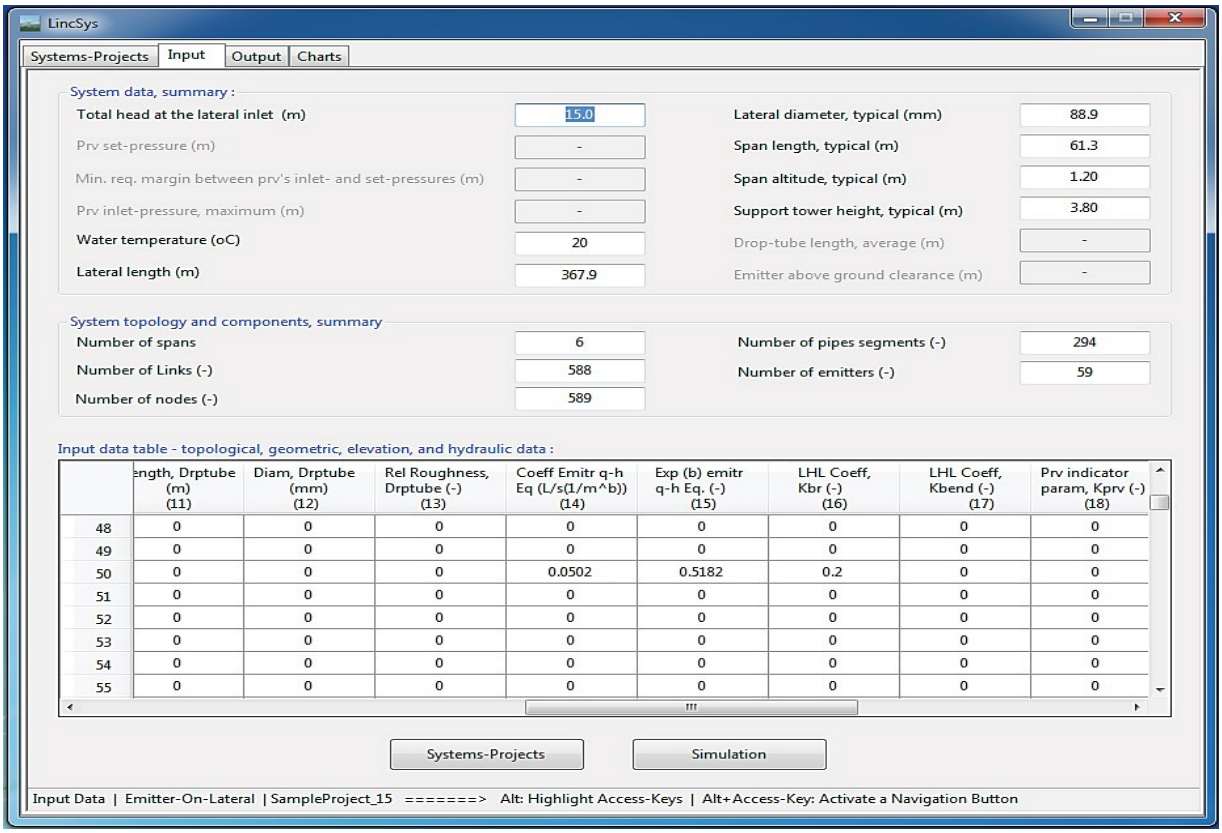

(a)

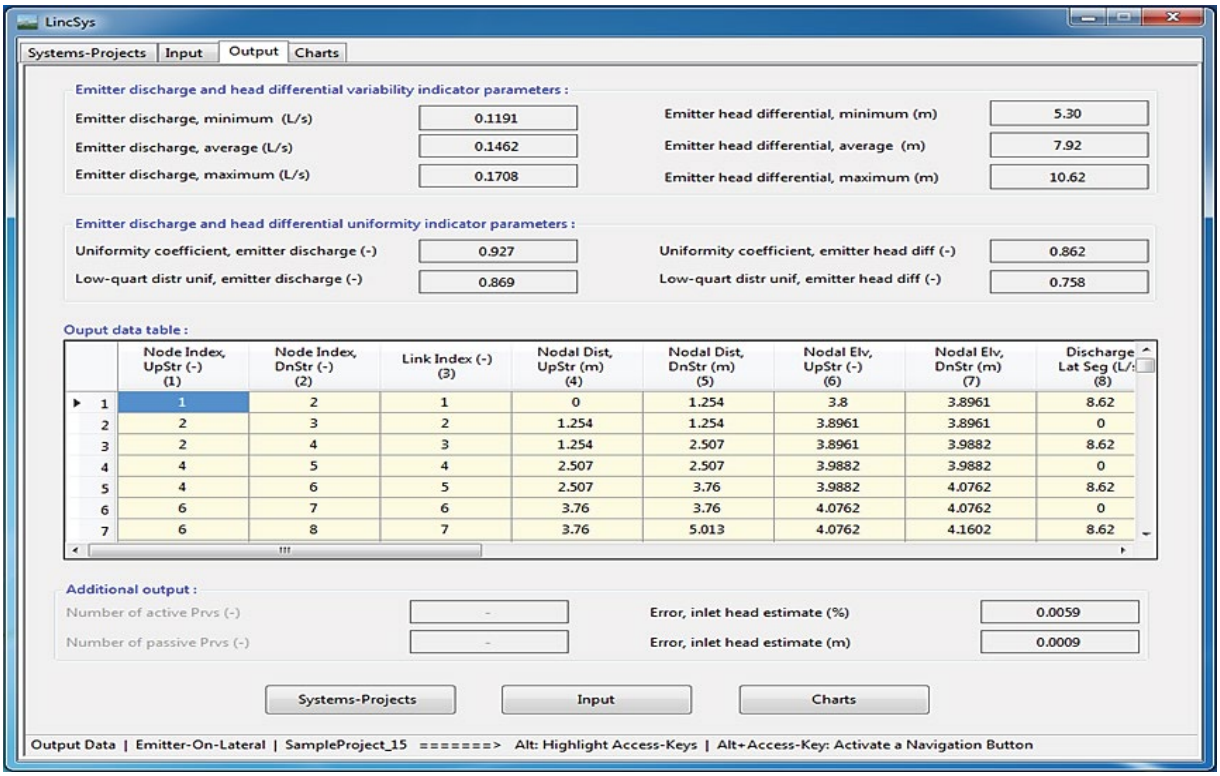

(b)

Figure 5. The Emitter-on-lateral sample project. (a) Input window and (b) output window

patterns for the current sample project are of the same general form as those of the corresponding lateral pressure profile variability patterns. Given that (in the lateral considered here) emitters are placed directly on the lateral outlets, it can be observed that for each emitter, the emitter inlet pressure is nearly the same as the local lateral pressure. The implication is that the emitter discharge profile is a strong function of the lateral pressure profile, which explains the observed similarity in profile patterns between the lateral pressure and emitter discharge profiles.

Although the emitter discharge profile, shown in Figure 6c, has the same general form as that of the lateral pressure profile depicted in Figure 6b, a close look at Figure 6c, nonetheless, reveals that the local in-span variability patterns of the emitter discharge profile do not precisely follow that of the lateral pressure profile. This is particularly evident in sections of the lateral around some of the span joints (particularly the span joints that are near the upstream-end), where the change in the slope of the emitter discharge profile (Figure 6c) is not as sharp that of the pressure head profile (Figure 6b).

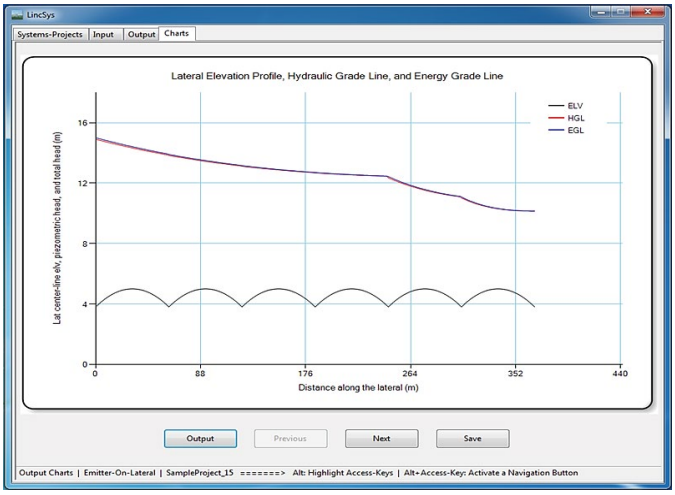

(a)

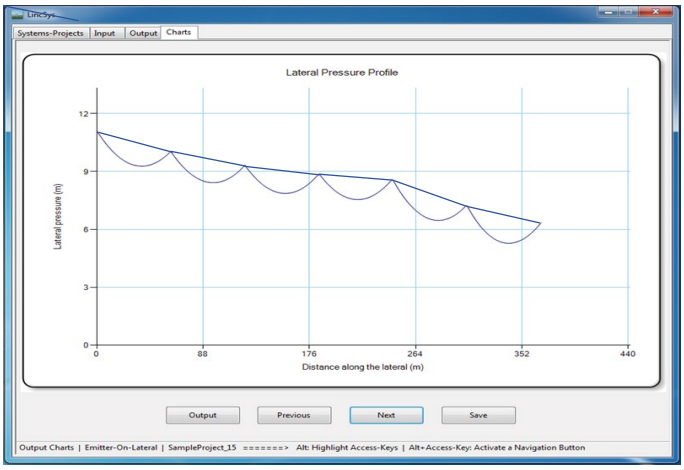

(b)

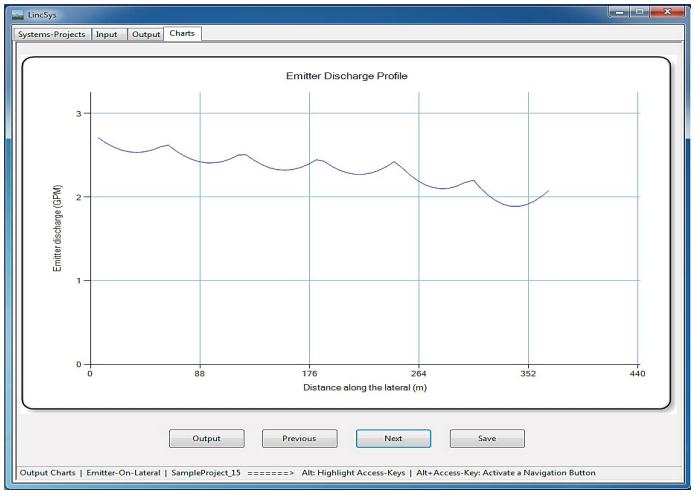

(c)

Figure 6. Charts of the emitter-on-lateral sample project. (a) Lateral elevation profile and hydraulic and energy grade-lines, (b) lateral pressure profile (the solid-line is the actual pressure head profile and the dash-dotted line depicts the inter-span variability trend) and (c) emitter discharge profile

The explanation for this observation is related to the significant differences in nodal spacing and outlet (emitter) spacing used in this lateral. While the average emitter spacing for the current lateral (a lateral that uses high pressure sprinklers) is set at about 6.24 m (Table 1), the nodal spacing was set to a constant value of 1.25 m along the lateral. Thus, the lateral pressure profile, evaluated at each of the computational nodes, has a sufficiently fine spatial resolution to track the form of the lateral elevation profile more closely. By contrast, the relatively large emitter spacings used in the current lateral meant that for at least some of the span joints (particularly the upstream-end span joints, Figure 6c) emitter placements are such that distances between the location of a span joint and those of the closest emitters are relatively large for the resultant emitter discharge profile to closely track the form of the lateral pressure profile near such a span joint. As a result, sections of the emitter discharge profile, about some of the span joints, appear not as sharp as the lateral pressure profiles.

Discussion

Simulation results presented earlier show that the hydraulic and the energy grade-lines, for the Droptube-Emitter and Emitter-On-Lateral sample projects, are decreasing functions of distance from the lateral inlet. This is the case for the Droptube-*Prv*-Emitter sample project as well, although the hydraulic and energy grade-lines chart for this project was not presented. Note that these observations are consistent with the fact that the laterals considered here are not equipped with a booster pump. In addition, the computed lateral pressure head profiles for each of the sample projects invariably show both local span-scale patterns and broader inter-span or lateral-wide trends, which is consistent results of earlier studies [12 and 13]. Evidently, this suggests that a complete description of the lateral pressure head profile variability patterns of these laterals requires that both spatial variability attributes be assessed.

The local in-span lateral pressure variability patterns are important, because they represent the spatial variability of the actual lateral pressure head profile for a given lateral hydraulic, geometric, and topographic parameter set. The significance of the inter-span lateral pressure variability trend, on the other hand, stems from the fact that it encapsulates the broader lateral-wide spatial variability attribute of the lateral pressure profile in the form of a curve with distinct monotonic property with respect to distance from the lateral inlet. The inter-span pressure variability trend can thus be a conveniently useful parameter in the analysis of the hydraulics of linear-move laterals as related to such variables as lateral dimeter and field slope.The in-span and inter-span lateral pressure variability attributes observed in the sample projects are primarily functions of span geometry. However, the simulation outputs presented earlier confirm results of earlier studies [13] that field slope and lateral diameter play the role of modifiers that damp out or amplify the basic convex/concave form of the in-span pressure profile variability patterns, and the associated in-span pressure differentials, produced by the span geometry. It is important to note here that these unique spatial variability attributes of the pressure head profiles of linear-move and center-pivot laterals are consistent with physically based reasoning and have also been confirmed by field data [12].

Simulated emitter discharge profiles show high degrees of uniformity, which is in line with levels reported by earlier studies [14]. The sample project outputs also show that, depending on the system configuration option, the emitter discharge profile variability attributes can have similarity with certain aspects of (or can be completely different from) the corresponding lateral pressure profile.

For the Droptube-Emitter system configuration option, the rather pronounced local span-scale wiggles of the lateral pressure head profile (Figure 2b), are substantially damped out in the corresponding emitter discharge profile (Figure 2c). As a result, only traces of the effects of in-span elevation differentials can be observed in the emitter discharge profiles. This is shown to be related to the position of emitters relative to the centerline of the lateral and the constant above ground clearance of emitters. By comparison, the lateral-wide emitter discharge profile has an analogous form to that of the corresponding inter-span lateral pressure profile (Figures 2b and 2c). This suggests that, for the Droptube-Emitter system configuration option, the inter-span lateral pressure variability trend can be a more useful indictor of the overall spatial variability attributes of the corresponding emitter discharge profile than the local in-span lateral pressure profile variability patterns.

For the Droptube-*Prv*-Emitter system configuration option, the emitter discharge profile (Figure 4c) exhibits distinctly different spatial variability patterns from that of the corresponding lateral pressure profile (Figure 4a). Furthermore, the emitter discharge variability pattern depends on whether a section of the lateral with active or passive *prvs* is being considered. Over a segment of the lateral in which *prvs* actively regulate pressure, emitter discharge profile (Figure 4c) is constant at a value determined by the *prv*-set pressure and hence local span-scale variability attributes are nonexistent. On the other hand, in a section of the lateral where *prvs* are operating in the passive mode (a section within which the emitters interact directly with the flow dynamics upstream of the *prv*), the emitter discharge profile show traces of local span-scale variabilities. Although the local span-scale variability of the emitter discharge profile is much less pronounced than the in-span variability levels of the corresponding lateral pressure profile, the overall emitter discharge profile variability trend is analogous in form to that of the corresponding inter-span lateral pressure profile variability trend (Figures 4a and 4c).

For the Emitter-On-Lateral system configuration option, on the other hand, the emitter discharge profile more closely tracks the in-span lateral pressure variability patterns (Figures 6b and 6c). The explanation for this lies in the fact that emitters are placed directly on lateral outlet ports and as a result emitter discharges are strong functions of the respective lateral outlet pressures.

Summary and Concluding Remarks

A software for simulating the hydraulics of linear-move and center-pivot irrigation systems, named *LincSys*, is presented in the current paper. This document is part II of a two-part article. Descriptions of software functionalities and capabilities relating to the GUI and also the physical and mathematical basis of the hydraulic simulation module of *LincSys* are presented in manuscript I. A brief summary of the results of a limited evaluation of the hydraulic simulation module (from an earlier study) and application examples (consisting of sample projects corresponding to each system configuration option of *LincSys*) are presented here.

A limited evaluation of the hydraulic module of *LincSys*, conducted based on a comparison of computed and measured lateral pressure head profiles, suggest that the predictive capability of the model is satisfactory. Furthermore, with the goal of highlighting the computational capabilities and the input-output functionalities of the software, simulated outputs of sample projects corresponding to each of the system configuration options of *LincSys* (i.e., Droptube-*Prv*-Emitter, Droptube-Emitter, and Emitter-On-Lateral) are presented here.

Corroborating results of earlier studies and in line with intuitive reasoning, computed pressure head profiles of linear-move and center-pivot laterals invariably exhibit both local span-scale patterns and broader inter-span or lateral-wide trends. Thus, a complete description of the pressure head profile patterns of linear-move and center-pivot laterals requires that both spatial variability attributes be assessed. Although the in-span and inter-span pressure variability properties are primarily functions of span geometry, the results presented here confirm the outcomes of earlier studies that field slope and lateral diameter modify the basic effects produced by the span geometry.

The computed emitter discharge profiles, of the sample projects, suggest that distribution uniformity along linear-move and center-pivot laterals can be high. The coefficient of uniformity of the simulated emitter discharges vary between a minimum of 0.927 and a maximum of 0.975 and the low-quarter distribution uniformity ranges between 0.869 and 0.969. Simulation results also show that, depending on the system configuration options, the emitter discharge profile variability attributes can have similarity with certain aspects of (or can be completely different from) the corresponding lateral pressure profile. For the Droptube-Emitter system configuration option, the lateral

pressure head profile exhibits pronounced local span-scale spatial variability patterns, which are substantially damped out in the corresponding emitter discharge profile. However, the emitter discharge profile exhibits lateral-wide variability trend that is analogous in form to that of the inter-span trend of the corresponding lateral pressure profile.

For the Droptube-*Prv*-Emitter system configuration option, on the other hand, the local in-span spatial variability attributes that are more pronounced in the lateral pressure profile are either lacking or are substantially damped out in the corresponding emitter discharge profile, depending on whether a section of the lateral with active or passive *prvs* is being considered. For the Emitter-On-Lateral system configuration option, on the other hand, the emitter discharge profile more closely tracks the in-span lateral pressure variability patterns and inter-span trends.

References

1. Kincaid, D.C and Heermann, D.F. "Pressure Distribution on a Center-Pivot Sprinkler Irrigation System." *Trans ASAE* 13 (1970): 556-558.
2. Chu, S.T and Moe, D.L. "Hydraulics of a Center Pivot System." *Trans ASAE* 15 (1972): 894-896.
3. Scaloppi, E. J and Allen, R.G. "Hydraulics of Center-Pivot Laterals. *J Irrig Drain Eng ASCE* 119 (1993): 554-567.
4. Anwar, A.A. "Friction Correction Factors for Center-Pivots." *J Irrig Drain Eng ASCE* 125 (1999): 280-286.
5. Tabuada, M.A. "Friction Head Loss in Center-Pivot Laterals with Single Diameter and Multidiameter." *J Irrig Drain Eng ASCE* 140 (2014): 04014033.
6. Valiantzas, J.D and Dercas, N. "Hydraulic Analysis of Multidiameter Center-Pivot Sprinkler Laterals." *J Irrig Drain Eng ASCE* 131 (2005): 137-146
7. Heermann, D.F and Stahl, K.M. CPED: Center Pivot Evaluation and Design. (2006).
8. Fraisse, C.W, Heerman D.F and Duke H.R. "Simulation of Variable Water Application with Linear-Move Irrigation System." *Trans ASAE* (1995): 1371-1376.
9. Keller, J and Bleisner R. "Sprinkle and Trickle Irrigation." Van Nostrand Reinhold, New York, NY (1990).
10. Martin, D.L, Denis C. K and Lyle, W.M. "Design and Operation of Sprinkler Systems." (eds. Hoffmann, G.J., Evans, R.G., Jensen, M.E., Martin, D.L., Elliott, R.L). *Design and Operation of Farm Irrigation Systems* (2nd Edn). MI, ASABE, St. Joseph. (2007): 557-631
11. Zerihun, D and Sanchez, C.A. "A software for hydraulic analysis of linear-move and center-pivot irrigation systems: LincSys, I. User interface and computational module." (2022).
12. Zerihun, D and Sanchez, C.A, Thorp, K.R and Hagler, M.J. "Hydraulics of linear-move sprinkler irrigation systems, III. Model evaluation." *Irrig Drainage System Eng* 8 (2019): 2.
13. Zerihun, D and Sanchez, C.A. "Pressure head profile of Linear-Move Sprinkler Irrigation Lateral: Analysis, Equation, and Profile Patterns." *Irrig Drainage System Eng* 8 (2019a): 239.
14. Keller, J, Corey F, Walker W.R and Vavra M.E. "Evaluation of Irrigation Systems. In Irrigation: Challenges of the 80's." Proc. St. Joseph, MI, ASAE. Second Nat'lIrrigation Symp (1980): 95-105.
15. Senniger.com. "Super Spray Customizable Field Proven Technology."(2017a). Retrieved from: https://www.senninger.com/sites/senninger.hunterindustries.com/files/super-spray-up3-brochure.pdf.
16. Senninger. "Pressure Regulator Guide." (2017b). Retrieved from:(https://www.senninger.com/sites/senninger.hunterindustries.com/files/pressure-regulator-guide.pdf).
17. Zerihun, D and Sanchez, C.A. "Hydraulics of linear-move sprinkler irrigation systems, I. System Description, Assumptions, and Definition of the Hydraulic Simulation Problem." *Irrig Drainage System Eng* (2019b): 236.
18. RainBird. "Agricultural Irrigation Products." (2020).
19. Granger, R.A. "Fluid Mechanics. Dover Publications Inc." New York, NY (1995).

How to cite this article: Zerihun D and Sanchez C.A. "A Software for Hydraulic Analysis of Linear-move and Center-Pivot Irrigation Systems: *LincSys*, II. Application Examples and Model Evaluation." Irrigat Drainage Sys Eng 11 (2022): 315.